Oxygen-Induced Restructuring of Rutile TiO$_2$(110): Formation Mechanism, Atomic Models, and Influence on Surface Chemistry

Min Li, Wilhelm Hebenstreit, Ulrike Diebold[#]

Department of Physics, Tulane University, New Orleans, LA 70118

Michael A. Henderson

Pacific Northwest National Laboratory, Richland, WA 99352

Dwight R. Jennison

Sandia National Laboratories, Albuquerque, NM 87185-1413

The rutile TiO$_2$(110) (1x1) surface is considered the prototypical 'well-defined' system in the surface science of metal oxides. Its popularity results partly from two experimental advantages: bulk-reduced single crystals do not exhibit charging, and stoichiometric surfaces - as judged by electron spectroscopies - can be prepared reproducibly by sputtering and annealing in oxygen. We present results that show that this commonly-applied preparation procedure may result in a surface structure that is by far more complex than generally anticipated.

[#] To whom correspondence should be addressed.
email: diebold@mailhost.tcs.tulane.edu

DISCLAIMER

DISCLAIMER

Portions of this document may be illegible in electronic image products. Images are produced from the best available original document.

Flat, (1x1) terminated surfaces are obtained by sputtering and annealing in ultrahigh vacuum. When re-annealed in oxygen at moderate temperatures (470 K to 660 K), irregular networks of partially-connected, pseudohexagonal rosettes (6.5 x 6 Å wide), one-unit cell wide strands, and small (~ tens of Å) (1x1) islands appear. This new surface phase is formed through reaction of oxygen gas with interstitial Ti from the reduced bulk. Because it consists of an incomplete, kinetically-limited (1x1) layer, this phenomenon has been termed 'restructuring'.

We report a combined experimental and theoretical study that systematically explores this restructuring process. The influence of several parameters (annealing time, temperature, pressure, sample history, gas) on the surface morphology is investigated using STM. The surface coverage of the added phase as well as the kinetics of the restructuring process are quantified by LEIS and SSIMS measurements in combination with annealing in ^{18}O-enriched gas. Atomic models of the essential structural elements are presented and are shown to be stable with first-principles density functional calculations. The effect of oxygen-induced restructuring on surface chemistry and its importance for TiO_2 and other bulk-reduced oxide materials is briefly discussed.

---

1 Introduction

The rutile $TiO_2(110)$ surface has evolved as one of the most important model systems for metal oxide surfaces. Titanium dioxide is used in gas sensing, catalysis, and photocatalysis, where surface phenomena play an important role. In 1994, when the surface science of metal oxides was reviewed by Henrich and Cox, $TiO_2(110)$ was already an intensely-studied system.[1] Since this time, its popularity has increased steadily, partly

because bulk single crystals can be reduced easily (which conveniently prevents charging), and partly because of the desire to perform experiments on a 'well-characterized system'.

The preparation of a clean, atomically flat TiO$_2$(110) (1 x 1) surface with a controlled defect density is very important for surface chemistry experiments. Normally, sputtering and annealing in ultrahigh vacuum (UHV) or oxygen at high temperatures are used. Many authors have published preparation recipes, as an example we cite the one given by Pan et al.:[2] "The stoichiometric (or nearly perfect) surface was obtained by sputtering with 500 eV Ar$^+$, then annealing to 1000 K for 3 min in 2x10^{-6} Torr of O$_2$, and finally cooling down to room temperature in the same oxygen atmosphere. XPS showed sharp Ti $2p$ peaks with no indication of reduced Ti states."

Most of the STM studies on TiO$_2$(110) performed so far [3-12] have focused on UHV annealed surfaces and the nature of the (1x2) reconstruction that evolves at high temperatures. Our STM measurements showed that oxygen-annealed surfaces prepared using Pan's recipe[2] were considerably rougher than vacuum-annealed samples, and that the appearance of the surface varied greatly when seemingly the same procedure was applied. In order to understand this phenomenon, we re-annealed flat surfaces (prepared by UHV annealing at high temperature) at moderated temperatures in oxygen gas, and found a pronounced morphology change we have termed restructuring. A brief report of STM results and conclusions was given previously,[13] and a more complete account (including data not shown here) will be published elsewhere.[14]

In this paper, we apply a combination of STM, LEIS and SSIMS to explore systematically the influence of preparation parameters (temperature, annealing time, oxygen pressure, and reduction state of the crystal) on surface restructuring. Ab-initio total-energy density functional calculations are used to test the geometric model for restructured surfaces, and

explore its electronic structure. As the main conclusion, we find that both the surface structure and morphology of a $TiO_2(110)$ surface depend sensitively on the oxidation conditions as well as the history of the crystal. Specifically, we find a new structure (termed 'rosette network') that consists of an incomplete $TiO_2(110)$ layer, where all atoms are in approximate bulk-like positions, but some are missing in a regular fashion. Compared to a (1x1) structure, the rosette networks exhibit quite different bonding geometry, coordination number, undercoordinated sites, and degree of covalency. Hence, $TiO_2(110)$ surfaces prepared by annealing in oxygen may not resemble the flat, (1 x 1) terminated surfaces that are often assumed in interpretation of surface chemistry experiments. With this work, we would like to provoke thoughts, and invite comments, on how surface chemistry may be affected by the presence of such rosette networks, and to what extent our findings may be transferable to other bulk oxide systems with facile transport of metal interstitials.

2 Experimental and calculation methods

The experiments were performed in two UHV systems described elsewhere.[15,16] Polished TiO_2 single crystals from three different vendors have been used which exhibited a blue color after an initial high-temperature anneal (950 K); details on sample mounting can be found in references [13-15]. Before each experiment, the sample was prepared with sputtering (1000 eV Ar^+, $I_{sample} \sim 8.3$ $\mu A \cdot cm^{-2}$, 20 min) and annealing to 880 K in UHV for 30 min which yielded a flat $TiO_2(110)$ (1 x 1) surface with atomically flat large terraces (up to 500 Å wide) as shown in Fig. 1. The alternating white and dark rows along the [001] direction are located at the positions of 5-fold coordinated Ti atoms and 2-fold bridging O atoms of the (1 x 1) structure, respectively.[11] Some bright rows typically several tens of nanometers long, are scattered across terraces or connected to step edges. These are appear upon UHV

4

annealing of relatively dark crystals.[17] In reference to the features observed upon annealing to higher temperature,[4-7] we call these rows (1 x 2) strands. Smooth step edges are oriented along the [1$\bar{1}$1] and the [001] direction.[12] Only Ti and O signals were detected by XPS and LEIS, indicative of a clean sample surface after such a treatment, and LEED showed a sharp (1 x 1) pattern.

Both pure $^{16}O_2$ gas and isotopically enriched $^{18}O_2$ gas ($^{18}O_2$:$^{16}O_2$ = 93% : 7%) were employed in oxygen exposure experiments. Gas dosing was performed by backfilling the chamber. To quantify the ^{18}O surface content, we took LEIS spectra[14] which show clearly separated ^{18}O and ^{16}O peaks. These LEIS measurements do not affect the uptake of ^{18}O with carefully controlled parameters (total ion fluence of ~ 1.6×10^{-15} cm^{-2} per measurement and beam energy of 1000 eV). Static SIMS experiments were performed in a separate chamber[16] with a differentially pumped ion gun utilizing a 500 V Ar$^+$ beam with an ion flux in the nA/cm^2 regime. No ion current was measured at the sample without Ar flowing through the gun, even with a 10^{-6} torr chamber pressure of O_2. This indicates that virtually no O_2 entering the gun from the chamber was exposed to the crystal as ions. During a typical experiment, the total Ar$^+$ ion exposure was maintained below about 5% of a monolayer in order to minimize any potential effects due to sputter damage. Secondary ions generated by sputtering were monitored with a quadrupole-based Extrel C50 spectrometer.

The electronic structure calculations used the massively parallel Gaussian-based code QUEST (QUantum Electronic STructure)[18] and density functional theory in the local density approximation (LDA) as described in ref.[14,19]. Successful tests of computational accuracy included comparisons with the results of Ramamoorthy et al.,[20] who used a plane wave code and different pseudopotentials. Local densities of states are found by the

standard projection on the local Gaussian bases. Integrating these to the Fermi level then results in local electron populations having diagonal (same atom) and off-diagonal (interatomic) parts, which provide information on the degrees of ionicity and covalency in local interactions.

3   Results

3.1. Oxygen-induced change of surface structure

In the following, we present LEIS and STM results after re-annealing at various temperatures flat, UHV-annealed surface similar to the one displayed in Fig. 1. The following procedure was employed each time: sputtering, UHV annealing, lowering the sample temperature to the specified value, exposing to $^{18}O_2$ gas (1x10^{-6} mbar) for the specified time, and cooling in UHV to room temperature.

$^{18}O_2$ exposure at 500 K for 10 min produces bright features evenly distributed on the (1 x 1) substrate as shown in Fig. 2a Most features are assembled into short aggregates (~40 Å) roughly oriented along the [1 $\bar{1}$ 0] direction. In addition, a few scattered (1 x 1) islands (ca. 40 Å x 30 Å, marked by arrows in Fig. 2a) can be seen on top and in between the large (1 x 1) terraces. The step edges of the (1 x 1) terrace become more irregular as compared to a UHV-annealed surface (Fig. 1). After annealing in $^{18}O_2$ at 520 K (Fig. 2b), distinctly different morphological features appear on the large (1 x 1) terraces. Patches of a rosette-like networks[13] (labeled 'R', typically 30 Å wide and elongated along the [1 $\bar{1}$ 0] direction) dominate, see Fig. 4 below. Located in between are small (1 x 1) islands (typical size of 60 Å x 40 Å). In addition, some white clusters are found on top of the (1 x 1) islands. Fig. 2c (annealing at 550 K) shows an even rougher surface, consisting of many layers of

somewhat larger (1 x 1) islands (~80 Å x 60Å), partially connected to each other and roughly oriented along the $[1\bar{1}0]$ direction. Between and on top of these islands are network patches ('R') also elongated along the $[1\bar{1}0]$ direction. The flat (1 x 1) substrate (still discernible in Fig. 2b) can no longer be identified in this image. After annealing in O_2 at 660 K (Fig. 2d), the (1 x 1) phase dominates the surface. The (1 x 1) islands are connected to each other to form large (1 x 1) terraces with larger network patches (ca. 100 Å x 80 Å) appearing on top of terraces. STM results[14] from a sample annealed in $p_{18O_2} =$ 1 x 10^{-6} mbar at 660K for 5,10, and 20 min gave images very similar to the one displayed in Fig. 2d (10 min). (This justifies comparison between annealing at 10 min (Fig. 2 a-d) to somewhat longer annealing times at higher temperatures in Fig. 2e,f.)

Oxygen exposure at 710 K for 15 min leads to a dramatic morphological change (Fig. 2e) with much larger (1 x 1) islands and straight step edges (some of which are reconstructed as is observed on UHV annealed surfaces[12]). A number of [001]-oriented bright strands (typically 70 Å long) are distributed uniformly on top of (1 x 1) terrace and extend out of step edges across the lower terrace. An even higher annealing temperature (Fig. 2f) yields large, flat (1 x 1) terraces with a few white clusters and bright strands on top of the bright [001]-oriented rows (the Ti sites) of the substrate. (Such strands are also visible in the small scale image below (Fig. 4).

Annealing in $^{18}O_2$ leads to incorporation of ^{18}O into the sample surface. LEIS ^{18}O peak areas (after normalization of the total LEIS O signal to 100%) that correspond to the images displayed in Fig. 2 are shown in Fig. 3. The ^{18}O content increases with temperature, up to a maximum value of 75% for Fig. 2d. Concurrent with the transition to flat, larger (1x1) islands and the absence of rosette networks, the ^{18}O content decreases again.

All surface displayed in Fig. 2 exhibit a (1x1) LEED pattern. XPS results of an oxygen-annealed surface reveal no difference in the Ti 2p peak position or shape as compared to a surface annealed for 30 min in UHV at 880 K. This may be caused by insufficient sensitivity of our XPS-setup. Previous measurements[2,21] showed a shoulder indicative of Ti^{3+} species (attributed to oxygen vacancies) on UHV-annealed surfaces.

A small scale STM image of both network patches and (1 x 1) islands is shown in Fig. 4. The small isolated (1 x 1) island (ca. 60 Å x 30 Å) at the center is partially connected to network patches. The network is atomically resolved as arrays of inter-connected pseudo-hexagonal units (named rosette: 'R'). Usually, one rosette (marked in Fig. 4) is composed of six bright spots with a width equal to the substrate unit cell in $[1\bar{1}0]$ direction (6.5 Å) and twice as long as the substrate unit cell in [001] direction (2 x 3 Å). Some bigger rosettes composed of more than six bright spots appear occasionally. Incomplete rosettes are incorporated into the edge of (1 x 1) islands, but rosettes never appear within an island. The rosettes have the same height as the (1 x 1) terraces. The dark centers of the rosettes appear on top of the bright rows (on top of the 5-fold coordinated Ti atoms) of the underlying TiO_2 (1 x 1) layer. Structural models of these rosettes are presented below (Figs. 8 and 9).

Some short bright strands (ca. 10 Å long) are connected to or located between network patches and (1 x 1) islands. Usually one of the six bright spots is missing at the connection between a rosette and a strand. In a forthcoming paper,[22] we argue that the strands exhibit the same structure as the double ridges of the $TiO_2(110)(1x2)$ reconstruction.[7]

3.2. Kinetics of the restructuring process

A study of the initial ^{18}O incorporation with annealing time was performed using static secondary ion mass spectrometry (SSIMS) in a separate chamber. The sample was prepared by sputtering and annealing in $^{16}O_2$ (6.7 x 10^{-7} mbar) at the temperature range from 477 K to 815 K. The $^{16}O_2$ gas was pumped out, the chamber was backfilled with $^{18}O_2$ gas (6.7 x 10^{-7} mbar), and the $^{18}O_2$ was pumped out after 260 sec. During the whole procedure the ^{18}O surface content was monitored (Fig. 5). The ^{18}O uptake occurs more rapidly with increasing annealing temperature, and decreases again above 669 K. This is consistent with the LEIS results displayed in Fig. 3, where a maximum of ^{18}O surface content was found after annealing for 10 min at 710 K. From Fig. 5, the ^{18}O uptake rate was determined using a $(1 - \Theta)$ dependence. The rate increases quickly below 566 K, slows down, and decreases above 669 K. From these rates, the ^{18}O activation energy is estimated to be 19 kcal/mol.

The uptake rate is strongly dependent on crystal 'age' (i.e., reduction state)[17] 'Fresh', as-purchased TiO_2 crystals are transparent. With increasing numbers of sputtering/ annealing cycles, they change in color from light to dark blue to metallic grayish. This color change is caused by the creation of color centers in the bulk and can be used as a quantitative measure for the degree of bulk reduction. Fig. 6 shows that darker, more reduced samples incorporate ^{18}O at a much faster rate than lighter, more stoichiometric samples. Displayed in Fig. 7 are two $TiO_2(110)$ samples with a different degree of bulk reduction. (These samples were mounted next to each other on one sample platen and sputtered and annealed simultaneously to ensure exactly the same treatment. A more detailed and quantitative investigation of the relationship between sample color, type of bulk defects, and surface properties is currently underway.[17]) A drastically different appearance is visible in STM; annealing in oxygen a light blue sample (left in Fig. 7) shows basically a (1x1) surface

termination, whereas the much darker sample (Fig. 7, right) is quite covered with rosettes. Both samples incorptorate ^{18}O, however (Fig. 6).

4 Discussion

4.1 Geometric model for rosette-like network structure.

A model for the rosette network has already been presented in a previous paper.[13] The main features are shown in Fig. 8. It consists of an incomplete TiO_2 layer, where the O and Ti atoms are missing in a regular fashion, and all the remaining atoms are in bulk-like positions. In Fig. 8b two islands are placed onto a (1 x 1) surface, the left one representing a rosette network with missing atoms, and the right one the regular (1 x 1) structure. First consider the (1 x 1) island. Titanium atoms are drawn as small, white balls and oxygen atoms as dark balls. We chose this shading for easier comparison with STM images where Ti sites are generally imaged bright.[11] As visible in the side view, oxygen atoms at higher locations are shaded darker. For example, the bridging oxygen atoms covering every other Ti row in the regular (1 x 1) structure are shown as black balls. The (1 x 1) structure has a rectangular unit cell as outlined on the far right of Fig. 8. The four 6-fold coordinated Ti atoms on the corners of the unit cell are covered by bridging oxygen atoms, and only the center Ti (5-fold coordinated) is visible in STM.

Outlined (with full lines) on the (1 x 1) island in Fig. 8 is a hexagon connecting four 5-fold-coordinated Ti and three six-fold-coordinated Ti atoms (underneath the bridging oxygens). Suppose the two bridging oxygen atoms marked with crosses as well as the six-fold coordinated Ti atom in the center are missing. Then, one would end up with six Ti atoms arranged in a quasi-hexagon (which is 6.5 Å (one unit cell) wide and 6 Å (two unit cells) high, as observed in the experiment). Exactly these atoms are missing in the 'R' network

10

structure shown on in Fig. 4, which consists only of O and Ti atoms in bulk-like positions. So conversely, adding one TiO_2 unit into the hexagon (full-lines) of the network structure of Fig. 8 generates the regular (1 x 1) structure. A second kind of hexagon with Ti atoms at the corners is drawn with dashed lines on both islands of Fig. 8. Here, one TiO unit (one 6-fold-coordinated Ti atom at the center and two 'connecting' bridging oxygen atoms, counted as one oxygen atom, at the sides) is missing in the network structure. Hence, the rosette-structure is simply an incomplete $TiO_2(110)$ layer with some atoms missing.

4.2 Electronic structure calculations for a rosette on top of TiO_2(1 x 1) (110) surface.

To test the stability of the proposed rosette structure, we performed LDA calculations using the 258-atom supercell shown in Fig. 9. A single rosette with six Ti atoms and twelve O atoms is arranged on top of a TiO_2(1 x 1) (110) substrate. The bottom three TiO_2 layers ($3^{rd} - 5^{th}$ layer in Fig. 9b) were frozen at the bulk positions and the top two layers of TiO_2 and the rosette were allowed to relax geometrically by minimizing the force of each atom. Relaxations of selected atoms are illustrated in Figs. 9a and 9b.

The rosette shows substantial horizontal relaxations (between 0.1 Å - 0.6 Å, Fig. 9a) with a general tendency to collapse towards the center. From the side view (Fig. 9b), all Ti atoms (1-6) in the rosette relax downward by 0.3 Å. All inner O atoms (9,12,16,17) sink by 0.3 Å, while 15 and 18 sink slightly (0.1 Å). The other outer O atoms (7,8,10,11,13,14) rise by 0.4 Å. Thus, the rosette is shrinking and buckling to reach its equilibrium position. This results in a shortening of Ti-O bond lengths by 0.1 to 0.2 Å as compared to the bulk. With the rosette on top of the substrate, the relaxation of Ti and O

atoms in the first layer is similar to the first-principle calculations of the clean (1 x 1) (110) surface.[23] The existence of rosettes causes small relaxations in the second and third layers.

The local density of states (LDOS) of bulk atoms (O131 and Ti130, not labeled in Fig. 10b), first layer atoms (O35 and Ti19) and the DOS of rosette atoms (averaged O, Ti1, and Ti3) are shown in Fig. 10. In each case, the Ti states dominate the unoccupied conduction band and the O states the valence band, similar to other theoretical works on the TiO_2(1 x 1) (110) surface.[23-28] When interpreting our STM images (Fig. 4), we assumed that the Ti atoms in the rosette are also imaged bright. The results displayed in Fig. 10 justify this assumption. In the rosette, the empty Ti 3d states dominate the conduction band and from the theory of Tersoff et al,[29] the tunneling current is found to be proportional to the surface LDOS at the position of the tip.

The valence band width of rosette O atoms is narrower as compared to O atoms on the (1x1) surface and in the bulk, and its shape is also different. Such changes should clearly be visible in UPS valence band measurements, especially if performed under conditions where the photon energy is varied to increase sensitivity to Ti 3d-derived states.[30] The gap width for both O 2p and Ti 3d states in the rosette is wider than that in the bulk as shown in Fig. 10. When analyzing the off-diagonal LDOS of selected Ti-O pairs[14] (not shown here), we find a significant increase in the strength of covalent interaction between Ti and O atoms in the rosette as compared to the bulk. We believe that it is this interaction which broadens the gap, moving the local conduction band minimum higher as seen in Fig. 10.

4.3 Mechanism

Only a few previous accounts of oxygen-induced morphological and structural changes of TiO$_2$(110) have been given. A brief Letter has been published by this group.[13] Engel and co-workers have observed cross-linked row structures along the [1$\bar{1}$0] direction after annealing the TiO$_2$(110) (1 x 2) phase in oxygen (1 x 10^{-7} Torr) at 1000 K followed by heating in UHV.[3,4] Onishi et al.[9] observed hill-like structures when exposing the TiO$_2$(110) (1 x 1) surface to O$_2$ gas (~1x10^{-7} mbar) at 800 K. With time, these features were transformed into added rows and new (1 x 1) terraces. This is consistent with our STM results above 710 K (Fig. 2e) where only added strands and (1 x 1) terraces are visible. Onishi et al. proposed a re-oxidation scheme where Ti^{n+} (n≤3) interstitial atoms from the reduced bulk are diffuse to the surface where they react with O$_2$ gas to form hills, added rows and new terraces. Consumption of Ti interstitials by reaction with surface oxygen produces a concentration gradient that results in a net diffusion current of these Ti interstitials towards the surface. The same mechanism, i.e., segregation of Ti^{n+}, combined with reaction with gaseous oxygen, is responsible for the formation of rosettes, strands and (1 x 1) islands in our experiments. The rate of surface restructuring is affected by the surface concentration of both reaction partners, Ti interstitials and O$_2$ molecules. The Ti segregation rate depends on temperature (influencing diffusion to the surface), number of Ti interstitials (reduction state of the crystal), and the chemical potential of oxygen (the oxygen pressure).

The restructuring process can be regarded as the manifestation of reoxidation of a reduced crystal at the atomic scale. It results in the growth of additional TiO$_2$ layers at the surface with Ti coming from the reduced bulk and oxygen from the gas phase. The kinetic processes and energetics that govern nucleation, growth, and morphology of deposited films are well-studied.[31] This case is special; because one constituent of the newly-added

13

film comes from the bulk, the kinetics of bulk diffusion must be taken into account as well. (Extensive TiO_2 bulk studies[32-39] revealed titanium interstitial ions as well as oxygen vacancies in a reduced TiO_2 crystal. Bulk diffusion studies [40-48] and a recent SSIMS investigation[49] show that Ti interstitials are the major diffusive species in TiO_2 rutile and not O vacancies.) For heavily reduced crystals, the added features nucleate mainly on terraces as is visible from their random distribution in low-coverage images (Fig 2a). This suggests that Ti interstitials are driven out in vertical direction from the bulk to the surface, where they react with oxygen. Some step-flow growth occurs also as evidenced by the relatively rough step edges that develop already at low temperatures and/or gas exposures. Step-flow dominates the growth on less reduced, light crystals (Fig. 7a).

The rosette networks are the precursors to the added (1 x 1) islands especially at lower temperatures (<660 K). The transition from rosettes to the (1 x 1) structure is straightforward as discussed above (section 4.1), one simply needs to add additional atoms to rosettes. This should happen easily upon arrival of new Ti interstitials on the surface, even without additional incorporation of O_2 from the gas phase. At low enough temperatures, the overall island shape of rosette network patches appear to be preserved during the transition to a (1 x 1) island, hence the preferred orientation of the (1 x 1) islands. When the temperature rises above ~ 700 K (Fig. 2e) the (1 x 1) islands assume a more square shape with step edge orientations typical for high-temperature UHV-annealed surfaces.[12]

There are three distinct regions for the rate of ^{18}O uptake, as reported in the context of Fig. 5. Initially, the rate increases with increasing temperature. At higher temperatures, a second process kicks in that first slows and then decreases the reaction rate with annealing temperature. This is also apparent in Fig. 3, where the total ^{18}O uptake for a given exposure time decreases above 700 K. Annealing an ^{18}O-rich surface in UHV decreases

14

the ^{18}O surface content, with a clear break point in the depletion rate around 740 K.[22] The ^{18}O can leave the surface via two routes: exchange with ^{16}O from the bulk, and desorption into the gas phase. The observed changes in surface morphology suggest that the latter process is dominant at high temperatures. Note that the slowdown in ^{18}O uptake under oxygen-rich conditions occurs concurrently with the disappearance of rosettes; upon annealing in $^{18}O_2$ at 710 K (Fig. 2e), only strands are formed on the surface. Similarly, rosettes transform into (reduced Ti_2O_3) strands when a ^{18}O-restructured surface is annealed in UHV at 690 K.[22] A mere scrambling between surface and bulk oxygen atoms cannot lead to a surface reduction. The assumption that desorption of oxygen from the surface occurs at temperatures above 700 K is also supported by other studies. It has been reported that surface point defects are created when $TiO_2(110)(1 \times 1)$ surfaces are annealed in UHV at temperatures above 700 K.[2] Xu et al.[10] observed a (1×2) reconstructed surface between 700-800 K, which reversibly converts to the (1×1) surface. They attributed this conversion to O desorption into the gas phase and/or Ti diffusion into the bulk. This is also consistent with our results; at temperatures above 830 K, only bulk-terminated (1×1) terraces exist (Fig. 2f), indicating that the row structure is also a metastable phase which converts into the most stable (1×1) terrace with temperature.

5.   Conclusion and open questions

Results presented in this paper clearly indicate that both the oxidation conditions and the history of the $TiO_2(110)$ sample have significant bearing on the morphology of the surface. It is somewhat frustrating that even this 'best characterized' of all metal oxide systems is not yet completely understood, and that characterization with spectroscopic and diffraction techniques is not sufficient to reveal the great differences in atomic structure that can form through annealing in oxygen. The STM images displayed in Fig. 7 are a good example.

Under exactly the same oxidation conditions, a very light blue crystal exhibits only a (1x1) structure, while a dark crystal is covered with rosettes. Hence, it is possible to deliberately prepare either a stoichiometric $TiO_2(110)(1x1)$ surface or one covered with the metastable structure.

The observed variations in the surface structure with O_2 pressure, crystal temperature and bulk defect density are so vast that we suspect chemistry of the $TiO_2(110)$ surface should be significantly variant for samples oxidized under different conditions. For example, the issue of whether water is molecularly or dissociatively adsorbed on $TiO_2(110)$[2,16,50-52] may be significantly clouded in the literature because of studies in which the morphology of the surface was unknowingly disordered by the presence of the rosettes and/or strands observed in this study by STM. Another example where restructured surfaces may exhibit quite different chemistry from a (1x1) surface is the adsorption of pyridine. Pyridine molecules bind more strongly at 4-fold coordinated Ti atoms at step edges as compared to the 5-fold coordinated Ti on the flat (1x1) surface as shown recently by Iwasawa's group.[53] Possibly, pyridine interacts strongly with rosette networks, where 4-fold coordinated Ti atoms are prevalent (Fig. 9). Metal overlayer film growth on $TiO_2(110)$ may be affected as well,[54] e.g., the roughness, induced by oxygen anneal of dark crystals, may influence nucleation and growth of overlayers. The rosette networks may also provide special adsorption sites for metal atoms, e.g., it is not inconceivable that one could place a single metal atom in the center of the rosette displayed in Fig. 9.

On a larger scale, the results in this study suggest that subsurface (interstitial) Ti is fairly labile in TiO_2 rutile, especially as the bulk concentration of these species increases. The bulk of small rutile particles could therefore act as sinks for excess Ti under reductive conditions, with this Ti returning to the surface under oxidative conditions. Such cycling of Ti between the bulk and surface should significantly influence surface properties of

small crystalline particles, as suggested by results in this work, but should also effect the bulk electrical and photoabsorptive properties.

Rutile $TiO_2(110)$ may not be the only system where such oxygen-induced morphology changes occur. A study of the reoxidation mechanisms of other bulk-reduced materials may provide an attractive playing field for surface scientists, where rich and interesting metastable structures may be expected.

6. Acknowledgment

References

1. V. E. Henrich and P. A. Cox, *The Surface Science of Metal Oxides*; Cambridge University Press, Cambridge, 1994.

2. J.-M. Pan, B. L. Maschhoff, U. Diebold and T. E. Madey, *J. Vac. Sci. Technol.*, 1992, **A(10)**, 2470.

3. A. Szabo and T. Engel, *Surf. Sci.*, 1995, **329**, 241.

4. M. Sander and T. Engel, *Surf. Sci. Lett.*, 1994, **302**, 263.

5. D. Novak, E. Garfunkel and T. Gustafsson, *Phys. Rev. B*, 1994, **50**, 5000.

6. P. W. Murry, N. G. Condon and G. Thornton, *Phys. Rev. B*, 1995, **51**, 10989.

7. H. Onishi and Y. Iwasawa, *Surf. Sci. Lett.*, 1994, **313**, 783.

8. H. Onishi, K. Fukui and Y. Iwasawa, *Bull. Chem. Soc. Jpn.*, 1995, **68**, 2447.

9. H. Onishi and Y. Iwasawa, *Phys. Rev. Lett.*, 1996, **76**, 791.

10. C. Xu, X. Lai, G. W. Zajac and D. W. Goodman, *Phys. Rev. B*, 1997, **56**, 13464.

11. U. Diebold, J. F. Anderson, K.-O. Ng and D. Vanderbilt, *Phys. Rev. Lett.*, 1996, **77**, 1322.

12. U. Diebold, J. Lehman, T. Mahmoud, M. Kuhn, G. Leonardelli, W. Hebenstreit, M. Schmid and P. Varga, *Surf. Sci.*, 1998, **411**, 137.

13. M. Li, W. Hebenstreit and U. Diebold, *Surf. Sci.*, 1998, **L414**, L951.

14. M. Li, L. Groß, W. Hebenstreit, U. Diebold, M. A. Henderson, D. R. Jennison, P. A. Schultz and M. P. Sears, *Surf. Sci.*, 1999, in print.

15. L. Zhang, M. Kuhn and U. Diebold, *Surf. Sci.*, 1997, **371**, 223.

16. M. A. Henderson, *Surf. Sci.*, 1996, **355**, 151.

17. M. A. Henderson, in preparation.

18. M. P. Sears and P. A. Schultz at Sandia National Laboratories, Albuquerque, NM 87185-1111.

19. C. Verdozzi, D. R. Jennison, P. A. Schultz, M. P. Sears, J. C. Barbour and B. G. Potter, *Phys. Rev. Lett.*, 1998, **80**, 5615; ibid. 1999, **82**, 799.

20. M. Ramamoorthy, D. Vanderbilt and R. D. King-Smith, *Phys. Rev. B*, 1994, **49**, 16721.

21. L. Wang, D. R. Baer and M. H. Engelhard, *Surf. Sci.,* 1994, **320**, 295.

22. M. Li, W. Hebenstreit and U. Diebold, in prepeparation.

23. K.-O. Ng and D. Vanderbilt, *Phys. Rev. B,* 1997, **56**, 10544.

24. O. Gülseren, R. James and D. W. Bullett, *Surf. Sci.,* 1997, **377-379**, 150.

25. S. Munnix and M. Scheits, *Phys. Rev. B,* 1984, **30**, 2202.

26. N. Yu and J. W. Halley, *Phys. Rev. B,* 1995, **51**, 4768.

27. D. Vogtenhuber, R. Podloucky, A. Neckel, S. G. Steinemann and A. K. Freeman, *Phys. Rev. B,* 1994, **49**, 2099.

28. D. Vogtenhuber, R. Podloucky and J. Redinger, *Surf. Sci.,* 1998, **402-404**, 798.

29. J. Tersoff and D. R. Hamann, *Phys. Rev. B,* 1985, **31**, 805.

30. Z. Zhang and V. E. Henrich, *Phys. Rev. B,* 1991, **43**, 12004.

31. J. A. Venables, *Surf. Sci.,* 1994, **299/300**, 798.

32. M. Aono and R. R. Hasiguti, *Phys. Rev. B,* 1993, **48**, 12406.

33. F. Millot, M. G. Blanchin, R. Tetot, J. F. Marucco, B. Poumellec, C. Picard and B. Touzelin, *Prog. Solid State Chem.,* 1987, **17**, 263.

34. P. Kofstad, *J. Less-Common Metals,* 1967, **13**, 635.

35. L. A. Bursill, M. G. Blanchin and D. J. Smith, *Proc. R. Soc. London A,* 1984, **391**, 373.

36. L. A. Bursill and D. J. Smith, *Nature,* 1984, **309**, 319.

37. J. Sasaki, N. L. Peterson and K. Hoshino, *J. Phys. Chem. Solids,* 1985, **46**, 1267.

38. H. B. Huntington and G. A. Sullivan, *Phys. Rev. Lett.,* 1965, **14**, 177.

39. D. J. Smith, L. A. Bursill and M. G. Blanchin, *Philisophical Magazine A,* 1984, **50**, 473.

40. D. J. Derry, D. G. Lees and J. M. Calvert, *J. Phys. Chem. Solids,* 1981, **42**, 57.

41. D. J. Neild, P. J. Wise and D. G. Barnes, *J. Phys. D,* 1972, **5**, 2292.

42. H. Kolem and O. Kanert, *Z. Metallkd.,* 1989, **80**, 227.

43. T. S. Lundy and W. A. Coghlan, *J. Phys. Colloq.,* 1973, 299.

44. K. Hoshino, N. L. Peterson and C. L. Wiley, *J. Phys. Chem. Solids,* 1978, **39**, 457.

45. D. A. Venkatu and L. E. Poteat, *Mater. Sci. Eng.,* 1970, **5**, 258.

46. J. R. Akse and H. B. Whitehurst, *J. Phys. Chem. Solids,* 1978, **39**, 457.

47. M. Arita, M. Hosoya, M. Kobayashi and M. Someno, *J. Amer. Ceram. Soc.,* 1979, **62**, 443.

48. M. Someno and M. Kobayashi, *Springer Ser. Chem. Phys.,* 1979, **9**, 222.

49. M. A. Henderson, *Surf. Sci.,* 1999, **419**, 174.

50. L. Wang, D. R. Baer, M. H. Engelhard and A. N. Shultz, *Surf. Sci.,* 1995, **344**, 237.

51. M. A. Henderson, *Langmuir,* 1996, **12**, 5093.

52. R. L. Kurtz, R. Stockbauer and T. E. Madey, *Surf. Sci.,* 1989, **218**, 178.

53. S. Suzuki, Y. Yamaguchi, H. Onishi, K. Fukui, T. Sasaki and Y. Iwasawa, *Catalysis Letters,* 1998, **50**, 117.

54. C. T. Campbell, *Surf. Sci. Rep.,* 1997, **27**, 1.

Figure captions:
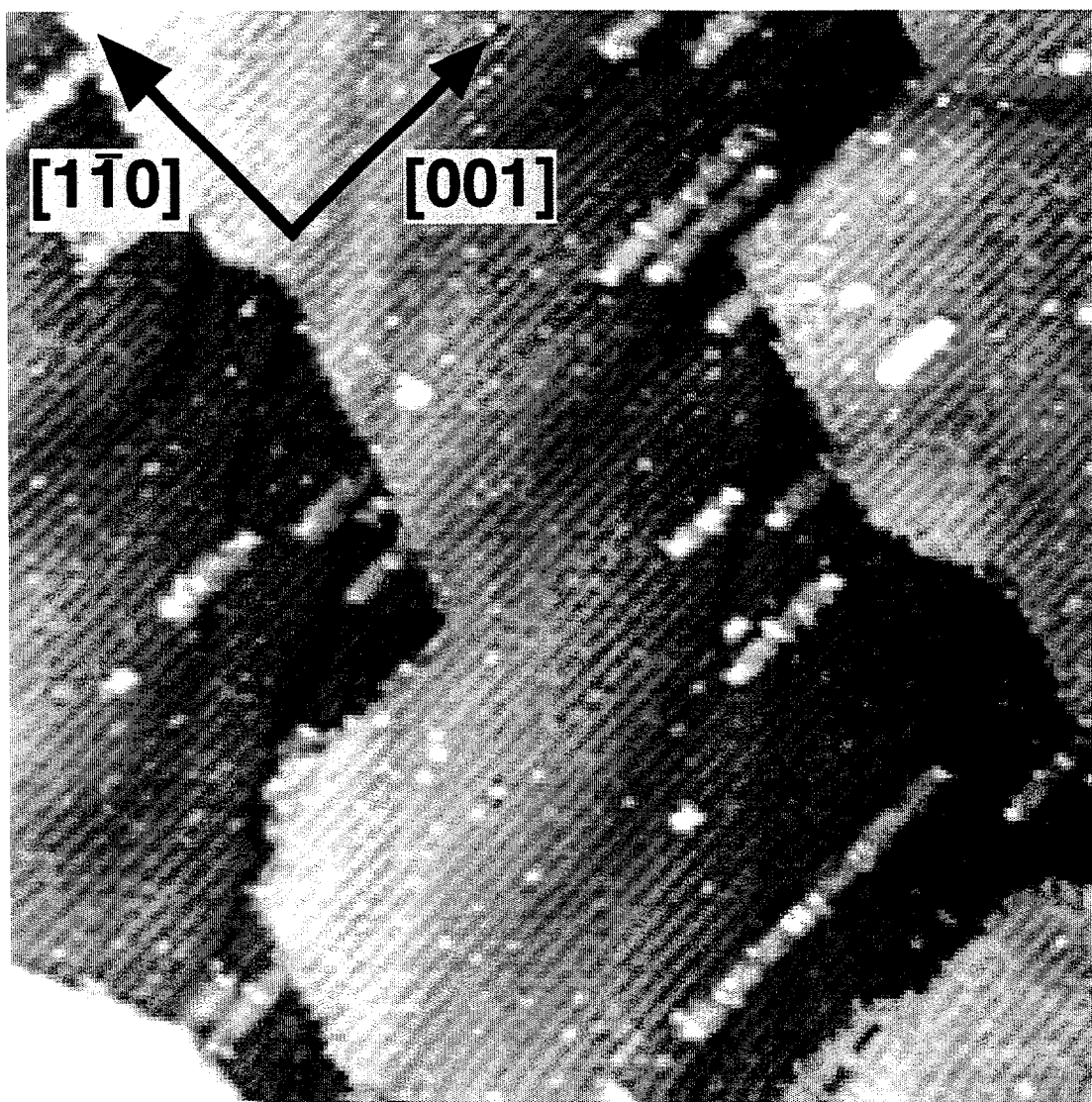
Fig. 1 STM image (500 Å x 500 Å) of TiO$_2$ (110), sputtered and annealed in UHV for 30 min at 880 K. The surface shows a regular (1 x 1) termination. The few bright lines are referred to as (1 x 2) strands.
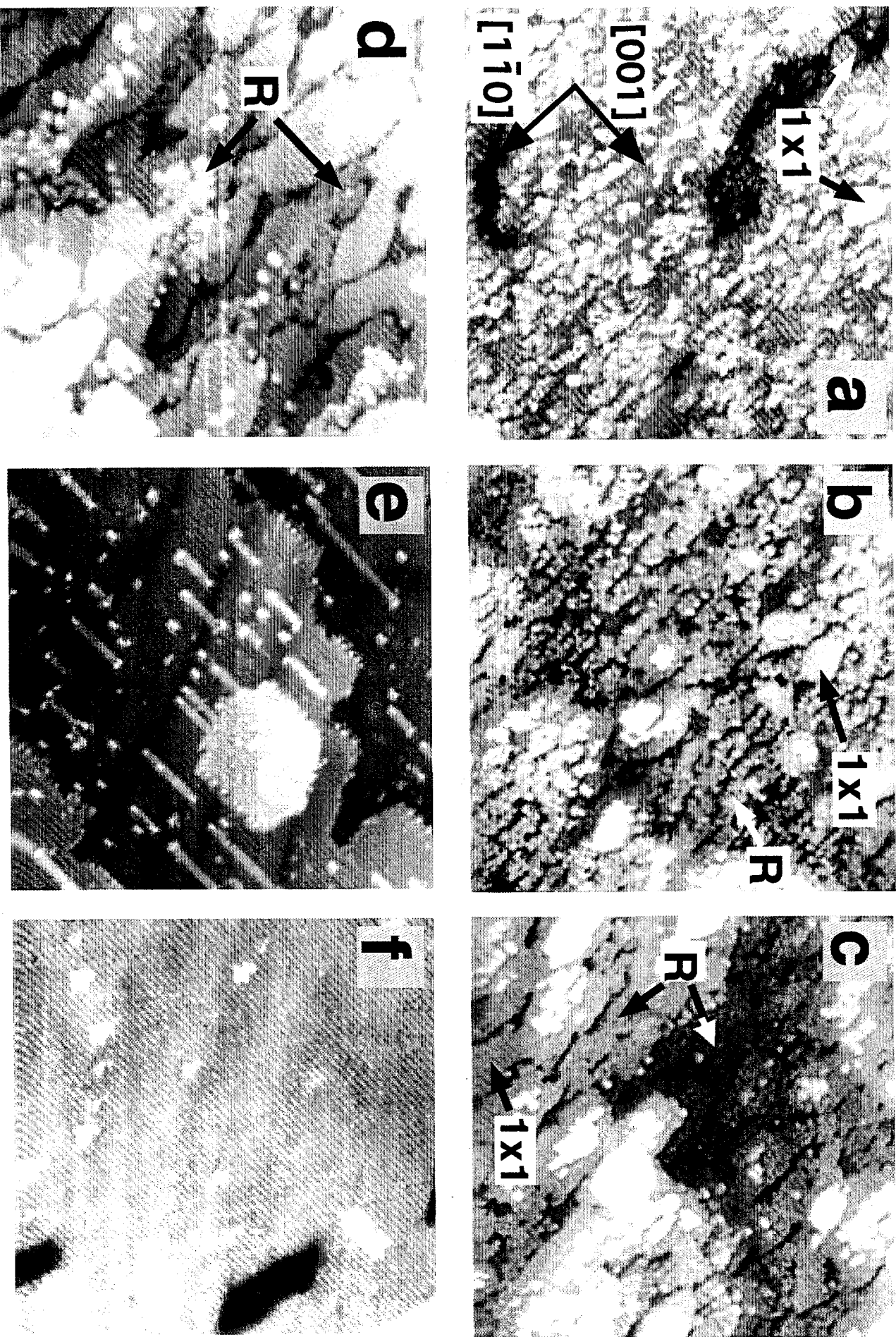
Fig. 2 STM images (500 Å x 500 Å) of a TiO$_2$ (110) surface. All surfaces were pretreated by sputtering and annealing in UHV at 880 K for 30 min. $^{18}O_2$ (1x10^{-6} mbar) was dosed at (a) 500 K, (b) 520 K, (c) 550 K, (d) 660 K for 10 min, (e) 710 K for 15 min, and (f) 830 K for 20 min.

Fig. 3 The surface concentration of ^{18}O (measured with LEIS) on TiO$_2$(110) surfaces prepared as in Figs. 2a~f.

Fig. 4 A small scale STM image (200 Å x 200 Å) of network patches ('R'), strands, and (1x1) islands after annealing in 1 x 10^{-6} mbar $^{18}O_2$ at 570 K for 25 min.

Fig. 5 The ^{18}O surface concentration during annealing in 6.7 x 10^{-7} mbar $^{18}O_2$ at various temperatures monitored with SSIMS.

Fig. 6 SSIMS of ^{18}O surface concentration during annealing in $^{18}O_2$ for rutile crystals with different colors. The color of a crystal is a measure of its bulk defect concentration.

Fig. 7 STM images (500 Å x 500 Å) of a light blue (a) and a dark (b) TiO$_2$(110) sample prepared by sputtering and UHV annealing at 970 K for 20 min followed by annealing in $^{18}O_2$ (1x10^{-6} mbar) at 570 K for 10 min.

21

Fig. 8 Atomic model (top and side view) for a restructured surface. A bulk-terminated
(1x1) island is shown on the right side. The network patch ('R') on the left side
consists of an incomplete $TiO_2(110)$ (1 x 1) layer and contains only atoms at bulk
positions. Small white balls are Ti atoms. Shadowed large balls represent oxygen
atoms, and darker shading indicates higher z-positions. The rectangle outlines the
unit cell of the (1x1) structure. The hexagons connect Ti atoms in similar positions
on both islands. Atoms missing in the network are marked with large crosses on the
(1 x 1) island.

Fig. 9 Supercell used for electronic structure calculations (a) top-view, (b) side-view.

Fig. 10 LDOS of selected atoms within the slab in Fig. 9.

Fig. 1 STM image (500 Å x 500 Å) of TiO$_2$ (110), sputtered and annealed in UHV for 30 min at 880 K. The surface shows a regular (1 x 1) termination. The few bright lines are referred to as (1 x 2) strands.

Fig. 2 STM images (500 Å × 500 Å) of a TiO_2 (110) surface. All surfaces were pretreated by sputtering and annealing in UHV at 880 K for 30 min. $^{18}O_2$ (1×10^{-6} mbar) was dosed at (a) 500 K, (b) 520 K, (c) 550 K, (d) 660 K for 10 min, (e) 710 K for 15 min, and (f) 830 K for 20 min.
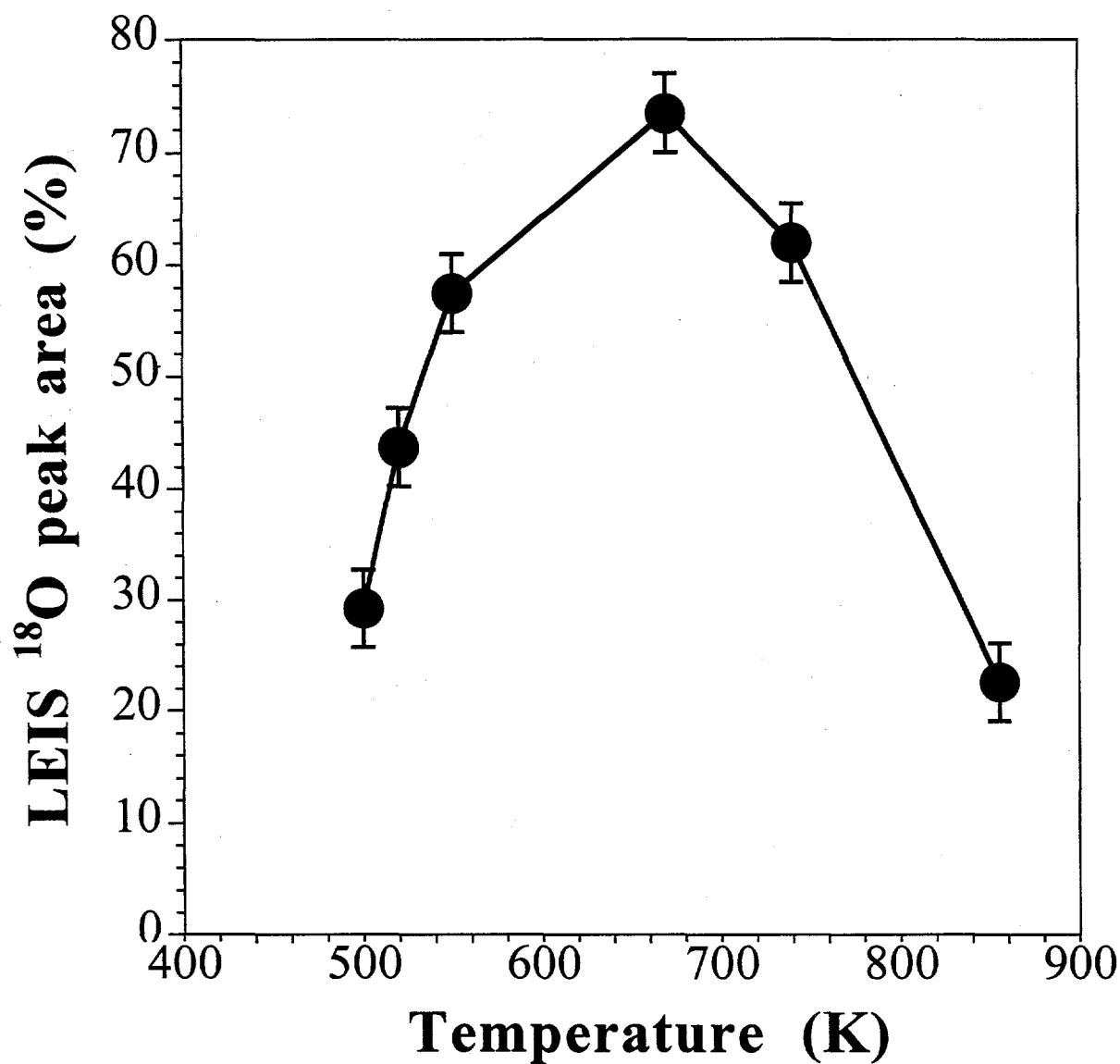
Fig. 3 The surface concentration of ^{18}O (measured with LEIS) on $TiO_2(110)$ surfaces prepared as in Figs. 2a~f.
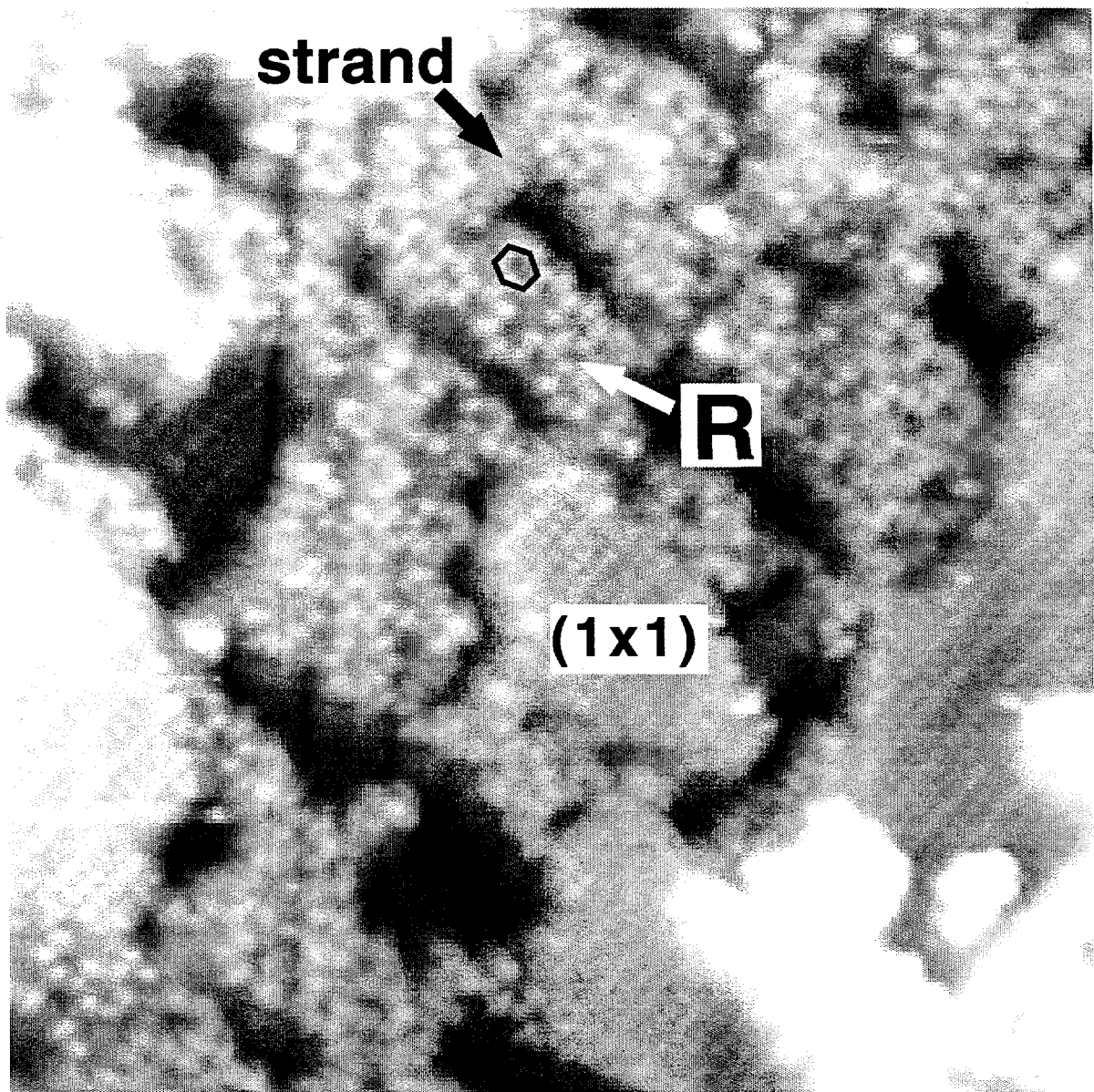
Fig. 4 A small scale STM image (200 Å x 200 Å) of network patches ('R'), strands, and (1 x 1) islands after annealing in 1×10^{-6} mbar $^{18}O_2$ at 570 K for 25 min.
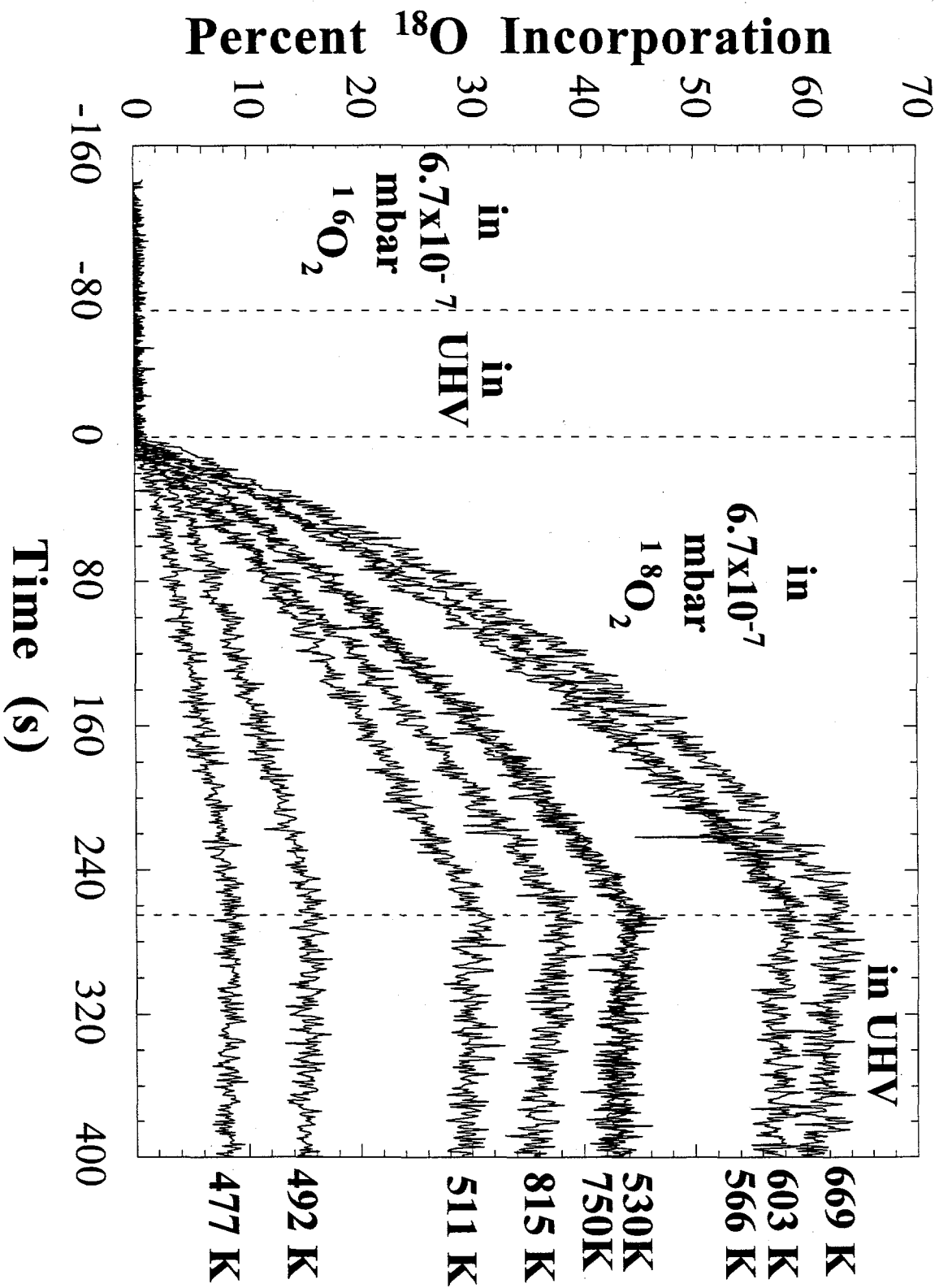
Fig. 5 The ^{18}O surface concentration during annealing in 6.7×10^{-7} mbar $^{18}O_2$ at various temperatures monitored with SSIMS.
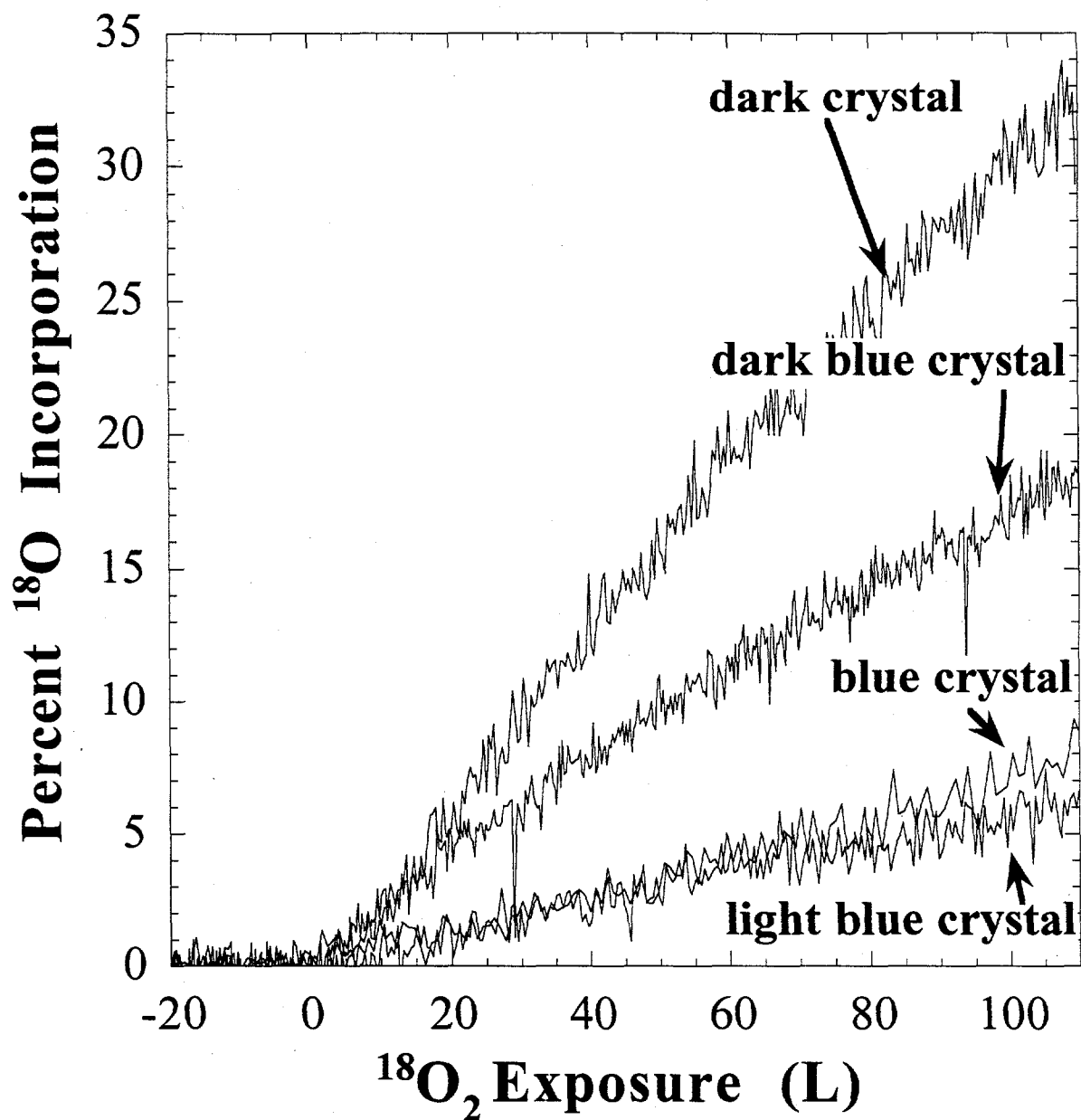
Fig. 6 SSIMS of ^{18}O surface concentration during annealing in $^{18}O_2$ for rutile crystals with different colors. The color of a crystal is a measure of its bulk defect concentration.
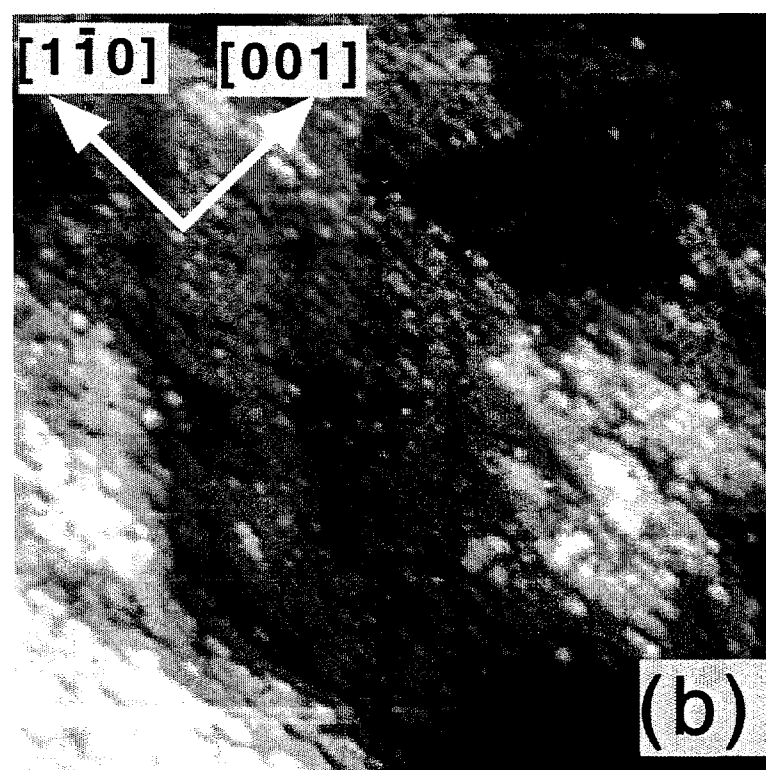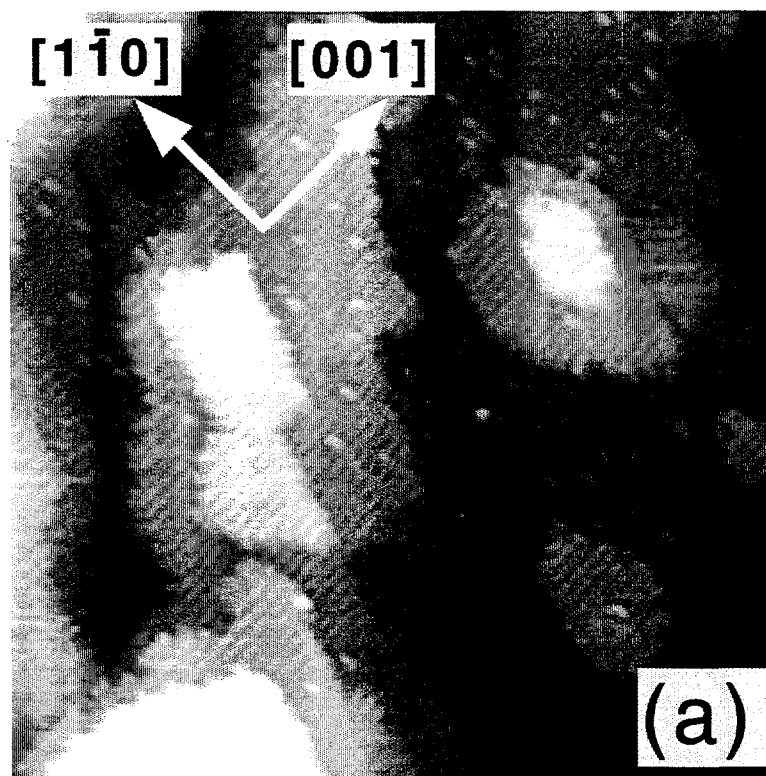
Fig. 7 STM images (500 Å x 500 Å) of a light blue (a) and a dark (b) TiO_2(110) sample prepared by sputtering and UHV annealing at 970 K for 20 min followed by annealing in $^{18}O_2$ (1×10^{-6} mbar) at 570 K for 10 min.
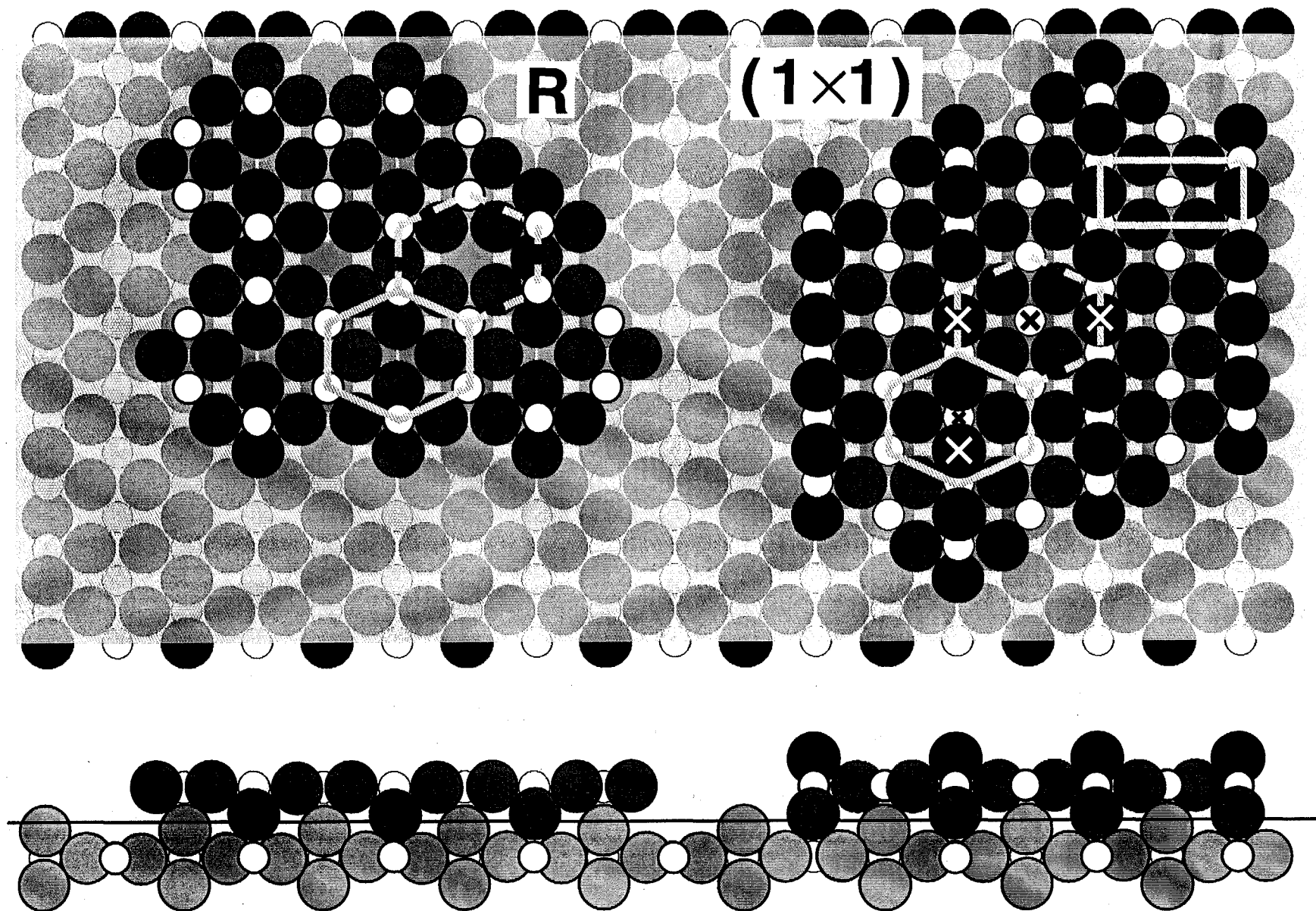
Fig. 8 Atomic model (top and side view) for a restructured surface. A bulk-terminated (1 x 1) island is shown on the right side. The network patch ('R') on the left side consists of an incomplete TiO_2(110) (1 x 1) layer and contains only atoms at bulk positions. Small white balls are Ti atoms. Shadowed large balls represent oxygen atoms, and darker shading indicates higher z-positions. The rectangle outlines the unit cell of the (1 x 1) structure. The hexagons connect Ti atoms in similar positions on both islands. Atoms missing in the network are marked with large crosses on the (1 x 1) island.
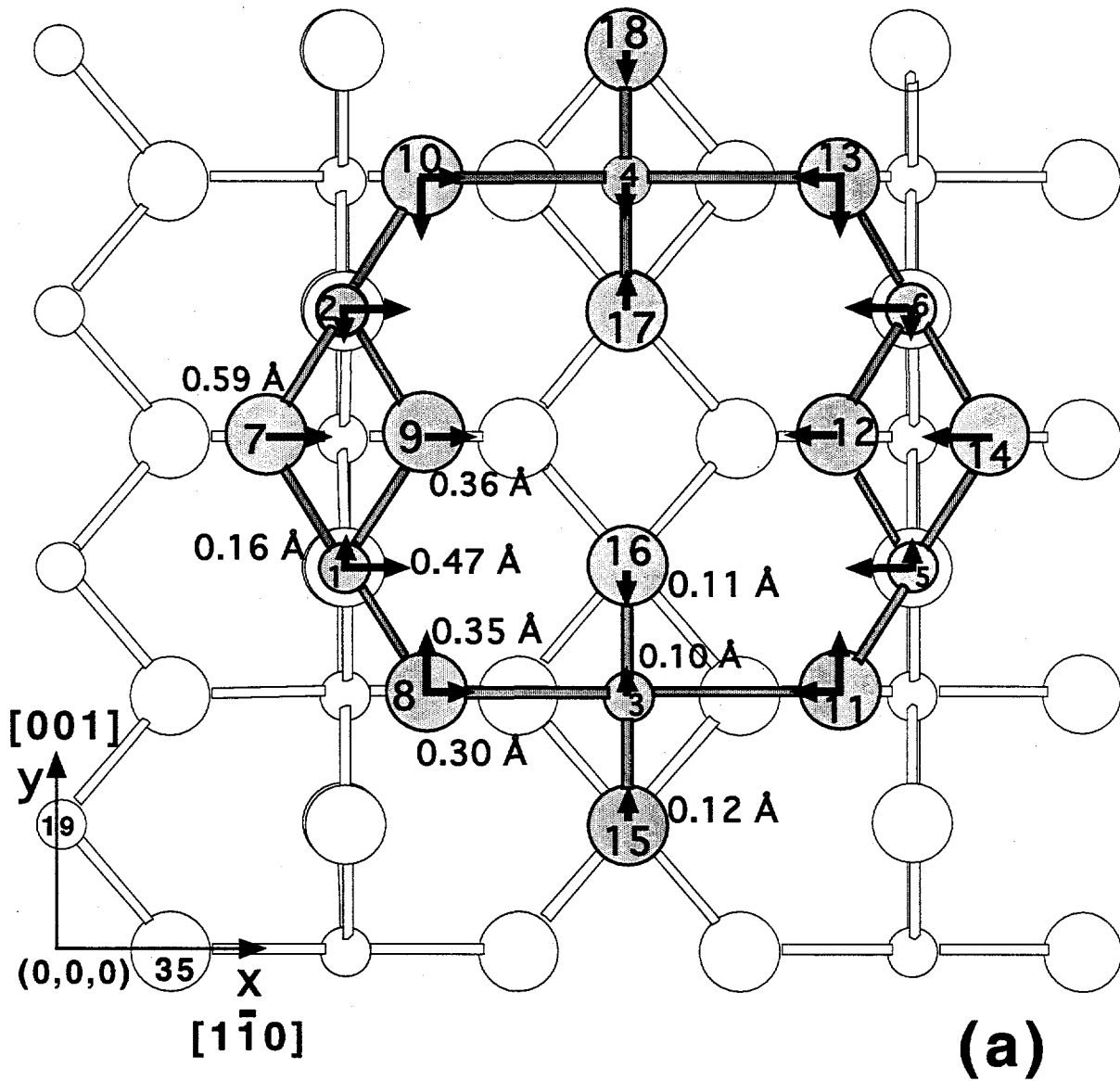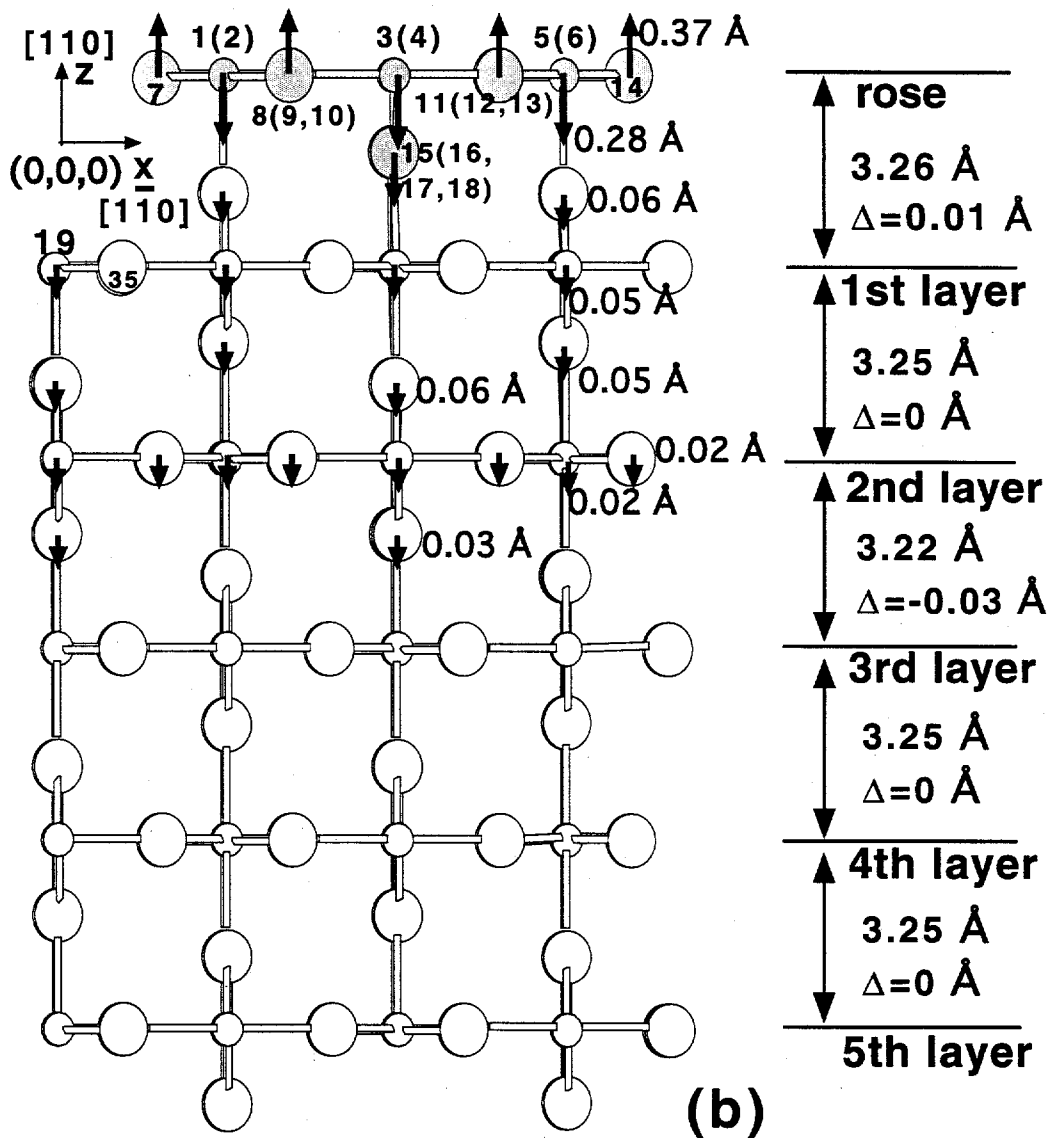
Fig. 9   Supercell used for electronic structure calculations (a) top-view, (b) side-view.

(b)

LDOS-O131 (bulk)

LDOS-T130 (bulk)

LDOS-O35 (1st layer)

LDOS-T19 (1st layer)

LDOS-O (rosette-average)

LDOS-Ti1 (rosette)

E_f

-6   -4   -2   0   2

Energy (eV)

(a)
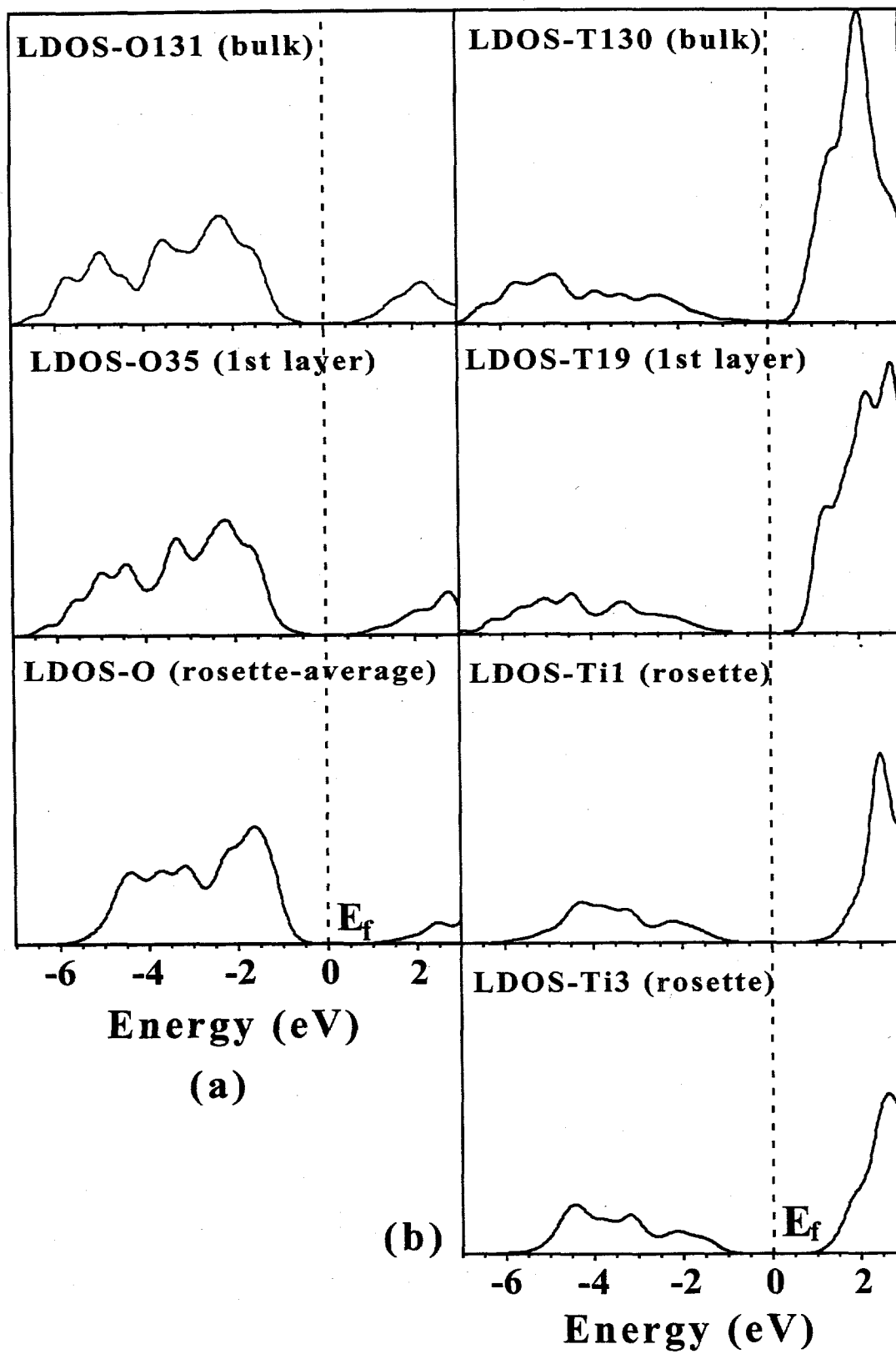
(b)

LDOS-Ti3 (rosette)

E_f

-6   -4   -2   0   2

Energy (eV)

Fig. 10 LDOS of selected atoms within the slab in Fig. 9.